Relevance of Human Aldoketoreductases and Microbial β-Glucuronidases in Testosterone Disposition[S]

Abdul Basit, John K. Amory, Vijaya Saradhi Mettu, Cindy Yanfei Li, ⬤Scott Heyward,
Parth B. Jariwala, Matthew R. Redinbo, and ⬤Bhagwat Prasad

*Department of Pharmaceutical Sciences, Washington State University, Spokane, Washington (A.B., V.S.M., B.P.);
Departments of Medicine (J.K.A.) and Pharmaceutics (C.Y.L.), University of Washington, Seattle, Washington; BioIVT Inc.,
Baltimore, Maryland (S.H.); and Departments of Chemistry, Biochemistry, and Microbiology and the Integrated Program for
Biological and Genome Sciences, University of North Carolina at Chapel Hill, Chapel Hill, North Carolina (P.B.J., M.R.R.)*

Received June 4, 2022; accepted December 6, 2022

ABSTRACT

Testosterone exhibits high variability in pharmacokinetics and glucuronidation after oral administration. Although testosterone metabolism has been studied for decades, the impact of UGT2B17 gene deletion and the role of gut bacterial β-glucuronidases on its disposition are not well characterized. We first performed an exploratory study to investigate the effect of UGT2B17 gene deletion on the global liver proteome, which revealed significant increases in proteins from multiple biological pathways. The most upregulated liver proteins were aldoketoreductases [AKR1D1, AKR1C4, AKR7A3, AKR1A1, and 7-dehydrocholesterol reductase (DHCR7)] and alcohol or aldehyde dehydrogenases (ADH6, ADH1C, ALDH1A1, ALDH9A1, and ALDH5A). In vitro assays revealed that AKR1D1 and AKR1C4 inactivate testosterone to 5β-dihydrotestosterone (5β-DHT) and 3α,5β-tetrahydrotestosterone (3α,5β-THT), respectively. These metabolites also appeared in human hepatocytes treated with testosterone and in human serum collected after oral testosterone dosing in men. Our data also suggest that 5β-DHT and 3α, 5β-THT are then eliminated through glucuronidation by UGT2B7 in UGT2B17 deletion individuals. Second, we evaluated the potential reactivation of testosterone glucuronide (TG) after its secretion into the intestinal lumen. Incubation of TG with purified gut microbial β-glucuronidase enzymes and with human fecal extracts confirmed testosterone reactivation into testosterone by gut bacterial enzymes. Both testosterone metabolic switching and variable testosterone activation by gut microbial enzymes are important mechanisms for explaining the disposition of orally administered testosterone and appear essential to unraveling the molecular mechanisms underlying UGT2B17-associated pathophysiological conditions.

SIGNIFICANCE STATEMENT

This study investigated the association of UGT2B17 gene deletion and gut bacterial β-glucuronidases with testosterone disposition in vitro. The experiments revealed upregulation of AKR1D1 and AKR1C4 in UGT2B17 deletion individuals, and the role of these enzymes to inactivate testosterone to 5β-dihydrotestosterone and 3α, 5β-tetrahydrotestosterone, respectively. Key gut bacterial species responsible for testosterone glucuronide activation were identified. These data are important for explaining the disposition of exogenously administered testosterone and appear essential to unraveling the molecular mechanisms underlying UGT2B17-associated pathophysiological conditions.

Introduction

Testosterone is an essential hormone that is important for male reproduction and the maintenance of secondary sexual characteristics, bone mineral density, and muscle mass. Testosterone masculinizing gender-affirming hormone therapy and testosterone replacement therapy are the frontline treatment options for transgender and hypogonadal men, respectively (Schlich and Romanelli, 2016; Spanos et al., 2020). Although >23 million Americans are seeking testosterone therapy, high interindividual variability in testosterone disposition is associated with high risk-to-benefit ratios (Bhasin et al., 2006; Bhasin et al., 2010; Swerdloff et al., 2015; Spanos et al., 2020). Variable testosterone pharmacokinetics (PK) can result in unpredictable side effects, including severe cardiovascular side effects (Bhasin et al., 2006; Bhasin et al., 2010; Schlich and Romanelli, 2016), which have led to a "black-box" warning issued regarding the testosterone label by the US Food and Drug Administration. Further, as urinary testosterone is used as a biomarker of testosterone doping, variable testosterone disposition is associated with inaccurate antidoping testing (Jakobsson et al., 2006; Schulze et al., 2008; Schulze et al., 2009; Strahm et al., 2015). Thus, variability in testosterone disposition presents critical challenges for the safe and effective gender-affirming hormone therapy

ABBREVIATIONS: AG, androsterone glucuronide; AGC, automatic gain control; AKR, aldoketoreductase; ALDH, aldehyde dehydrogenase; BSA, bovine serum albumin; DDA, data-dependent acquisition; DHCR, dehydrocholesterol reductase; DHT, dihydrotestosterone; EtioG, etiocholanolone glucuronide; GUS, β-glucuronidase; HI, hepatocyte incubation; OPLS-DA, orthogonal partial least squares discriminant analysis; PK, pharmacokinetics; TG, testosterone glucuronide; THT, tetrahydrotestosterone; UGT2B17, UDP-glucuronosyltransferase 2B17.

and testosterone replacement therapy as well as for accurate antidoping testing and enforcement.

Exogenously administered testosterone through oral, intramuscular, or topical routes shows significant interindividual variability in its PK irrespective of the route of administration (Mazer et al., 2005; Wilson et al., 2018). The variable testosterone PK is likely due to the involvement of polymorphic transport and elimination, release from the depot site, and/or prodrug activation as well as the first-pass metabolism and poor bioavailability (Rane and Ekström, 2012). Regarding testosterone metabolism, 17β-hydroxysteroid dehydrogenases (17β-HSDs), 5α-reductases, and UDP-glucuronosyltransferase 2B17 (UGT2B17) play important roles in converting testosterone to its primary metabolites, androstenedione, dihydrotestosterone (DHT), and testosterone glucuronide (TG), respectively (Fig. 1) (Basit et al., 2018). We have shown that testosterone and its secondary but major inactive unconjugated metabolites (androsterone and etiocholanolone) are primarily metabolized by glucuronidation (Basit et al., 2018), where the average serum concentration time (area under the curve) profiles of TG, androsterone glucuronide (AG), and etiocholanolone glucuronide (EtioG) are 80-, 380-, and 85-fold higher than the unconjugated testosterone after 800-mg oral testosterone dosing.

UGT2B17 is a highly variable human testosterone-metabolizing enzyme. Copy number variation and single-nucleotide polymorphisms as well as nongenetic factors (age and sex) are associated with variable UGT2B17 expression and activity (Bhatt et al., 2018; Zhang et al., 2018). Interestingly, the distribution of UGT2B17 copy number variation shows a high population variation, with deletion frequencies ranging from ~15% in Nigerians to >90% in the Japanese population (Xue et al., 2008). UGT2B17 deletion is linked to diseases such as prostate cancer (Kpoghomou et al., 2013; Gauthier-Landry et al., 2015), osteoporosis, and obesity (Zhu et al., 2015). The urinary excretion of

testosterone as a glucuronide is reduced by 90%, a significant change, in UGT2B17 deletion subjects compared with UGT2B17 high expressers (Jakobsson et al., 2006; Juul et al., 2009). However, the serum testosterone concentration in the deletion group is only 15% higher when compared with UGT2B17 expressers (Yang et al., 2008). We hypothesize that this discrepancy is likely due to the presence of other, potentially compensatory metabolic pathways in the UGT2B17 deletion group.

We have also shown previously that TG formed in the liver and intestine can be eliminated into bile, intestinal lumen, or blood through multidrug resistance-associated proteins MRP2 and MRP3 (Li et al., 2019), and organic anion transporting polypeptide (OATP1B) transporters can uptake TG into the liver (Li et al., 2020). These data suggest that TG elimination to bile and intestine is more favored over its transport into the blood. Because glucuronide metabolites are generally activated by bacterial β-glucuronidase (GUS) enzymes present in commensal microbiota (Ervin et al., 2019), we hypothesized that the high concentrations of serum androgen glucuronides are likely deconjugated to their respective unconjugated forms. Although AG and EtioG represent inactivation pathways in testosterone metabolism, TG and dihydrotestosterone glucuronide (DHTG) could be reactivated to testosterone and DHT through the actions of bacterial GUS proteins. Consistent with our hypothesis, a recent study showed that high concentrations of free DHT are found in the colonic contents of specific pathogen-free mice but are not observed in germ-free mice (Colldén et al., 2019). Thus, it is important to investigate the interplay between various mechanisms of testosterone inactivation and reactivation catalyzed by both human and gut microbial gene products.

The first aim of this study was to investigate the association of UGT2B17 gene deletion with the liver proteome. The hypothesis-generating proteomics data revealed upregulation of unique androgen metabolic
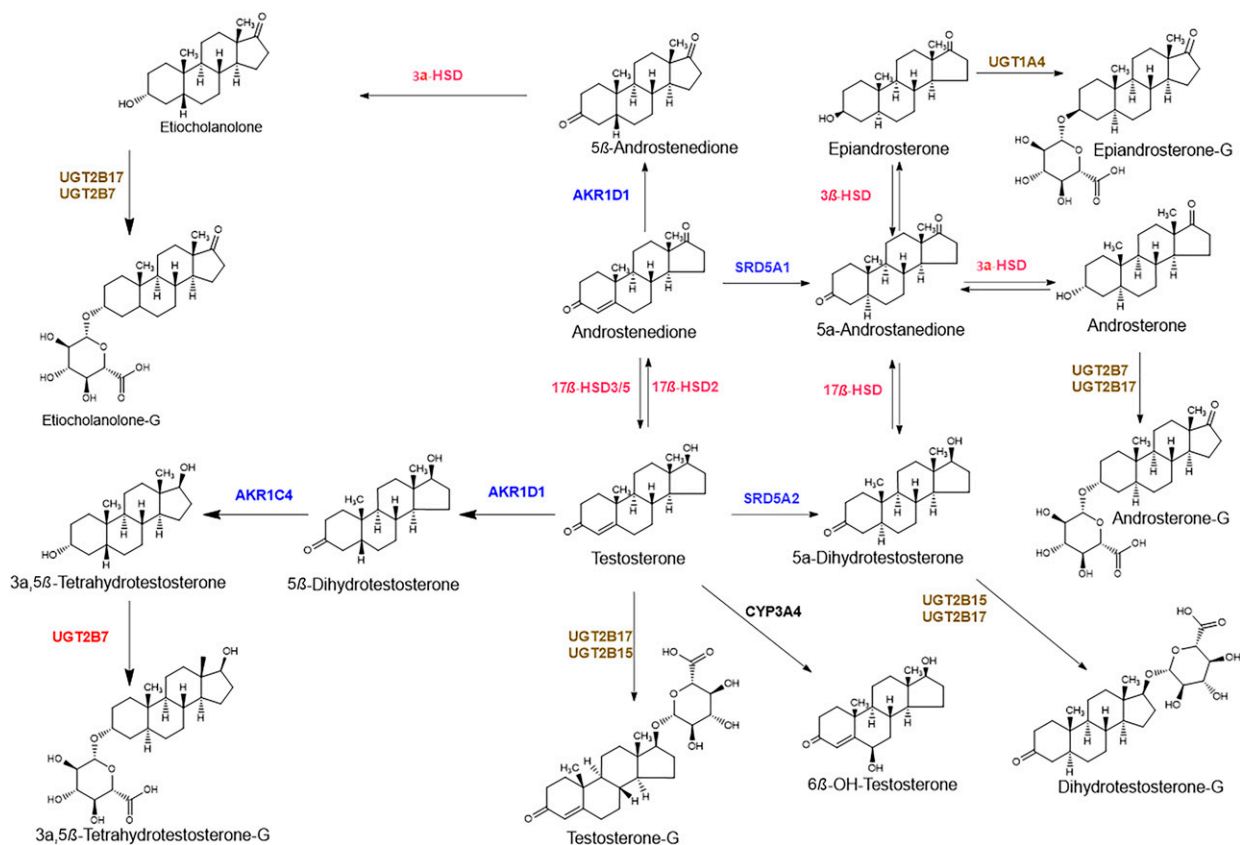

Fig. 1. Testosterone metabolism scheme in the gene deletion and the high expressers of UGT2B17.

pathways, which were then evaluated through a series of in vitro and in vivo data. Second, we characterized the potential gut microbial GUS enzymes that can activate TG into testosterone.

Materials and Methods

Materials

Steroid and steroid conjugate standards were purchased from either Cerilliant Corp (Round Rock, TX) or Steraloid (Newport, RI). Liquid chromatograhy tandem mass spectrometry (LC-MS/MS)–grade acetonitrile, methanol, acetone, and formic acid were procured from Fisher Scientific (Fair Lawn, NJ). Recombinant human UGT2B7, UGT2B15, and UGT2B17 Supersomes were purchased from Corning Inc. (Corning, NY). Trypsin, iodoacetamide, dithiothreitol, and bovine serum albumin (BSA) were purchased from Thermo Fisher Scientific (Rockford, IL). Ammonium bicarbonate (98% purity) was purchased from Acros Organics (Geel, Belgium), whereas alamethicin, cofactor UDP-glucuronic acid, magnesium chloride, and di- and monobasic potassium phosphate was purchased from Sigma-Aldrich (St. Louis, MO). Custom synthesized surrogate peptides for targeted proteomics analysis were procured from Thermo Fisher Scientific. Cryopreserved primary human hepatocytes ($n = 4$) as well as hepatocyte thawing and hepatocyte incubation (HI) media were kindly provided by BioIVT Inc. (Baltimore, MD). Liver S9 fraction and cytosol samples were procured from liver tissues procured from the Human Liver Bank of University of Washington School of Pharmacy (Seattle, WA) in our previous study (Bhatt et al., 2018).

Untargeted Proteomics Analysis of Liver S9 Fraction

Sample Preparation and LC-MS/MS Acquisition. S9 fraction was isolated from previously genotyped UGT2B17 deletion ($n = 3$; two males and one female) and high-expressing ($n = 3$; all males) liver samples for untargeted proteomics assay (Bhatt et al., 2018). The total protein concentration was determined with bicinchoninic acid assay, and 80 μL (2 mg/mL) S9 fraction was transferred for trypsin digestion using a previously optimized method (Balhara et al., 2021). Briefly, the sample was mixed with 10 μL BSA (0.2 mg/mL) and reduced using 10 μL dithiothreitol (250 mM) at 95°C for 10 minutes. After cooling the sample for 10 minutes, the denatured protein was subjected to alkylation using iodoacetamide (500 mM, 20 μL) in the dark at room temperature. The protein sample was precipitated with 1 mL ice-cold acetone followed by centrifugation at 16,000g and 4°C for 10 minutes. The pellet was collected, dried at room temperature (10 minutes), and washed with 0.5 mL ice-cold methanol. After centrifugation at 8000g, the protein pellet was collected, dried for 30 minutes at room temperature, and redissolved in 50 mM ammonium (60 μL) bicarbonate for trypsin digestion using 20 μL of trypsin solution (trypsin to protein ratio 1:100) at 37°C for 16 hours. The reaction was quenched with 5 μL 5% formic acid and centrifuged at 8000g (4°C for 5 minutes).

Tryptic peptides from the liver S9 fraction were analyzed in data-dependent acquisition (DDA) mode using Q-Exactive HF MS coupled with EASY-nLC 1200 system (Thermo Fisher Scientific, Waltham, MA). The tryptic digest (0.9 μg protein) was loaded onto a Thermo Scientific Acclaim PepMap 100 C18 HPLC column with a mobile phase [0.1% formic acid in water (A) and 0.1% formic acid in acetonitrile (B)] at a flow rate of 0.3 μL/min. The following gradient program was used: 5% B (0–5 minutes), 5%–25% B (5–105 minutes), 25%–40% B (105–125 minutes), 40%–95% B (125–126 minutes), and 95% B (126–136 minutes). The column temperature was 40°C.

mass spectrometry data were acquired using the DDA approach using top 10 ions (m/z range, 375–1500) from the survey scans. The full MS scanning was performed with automatic gain control (AGC) target set to 3e^6 and a higher energy collisional dissociation fragmentation with an AGC value of 1e^5. The isolation of the precursors was performed with a 1.6 m/z window. The survey scans were performed at a resolution of 120,000 (at m/z 200), whereas the resolution for higher-energy C-trap dissociation spectra was set to 15,000 (at m/z 200) with a maximum ion injection time of 35 milliseconds. The fragmentation was performed at the normalized collision energy of 27 eV. The precursor ions with single, unassigned, or six and higher charge states were excluded from the fragmentation.

Analysis of Untargeted Proteomics Data. The DDA data were processed with MaxQuant version 1.6.8.0 (Max-Planck Institute for Biochemistry, Planegg, Germany) using Andromeda search engine (Tyanova et al., 2016a), in which the high-resolution MS/MS spectra were searched against the human liver proteome database (15,656 proteins) curated from UniPort (www.uniprot.org). A decoy database constructed within MaxQuant was employed to control the false discovery rate. Trypsin was selected as the proteolytic enzyme with a maximum of two missed cleavages. Carbamidomethylation of cysteine was selected as a fixed modification, and N-terminal acetylation and methionine oxidation were selected as variable modifications. Peptides were searched with the mass tolerance of 5 ppm (at MS1 level) and 10 ppm (at MS2 level). Both peptide and protein false discovery rate were set to a maximum value of 1%. Only surrogate (unique) peptides were selected for the protein quantification based on label-free quantitation. The MaxQuant data were processed using Perseus software (1.6.8.0) (Tyanova et al., 2016b), where the following hits were first removed: contaminants, proteins identified by the reverse sequence, and proteins identified in only one replicate out of three (ambiguous identification). Principal component analysis of the shortlisted data were performed to identify the group-dependent clustering of the replicates and to visualize if the liver proteome is different between two groups (UGT2B17 deletion versus high expressers). Further orthogonal partial least squares discriminant analysis (OPLS-DA) analysis was performed for the two groups, which was used to identify proteins significantly different in these groups by S-plot. The differentially expressed proteins obtained from S-plot with a P value <0.05 were subjected to pathway analysis using STRING (Szklarczyk et al., 2015). The protein interactome was generated with a list of both upregulated and downregulated protein to characterize the protein-protein interactions and associated molecular and biologic pathways by the functional protein association network analysis using STRING database (https://string-db.org).

Characterization of Alternate Testosterone Metabolism Pathways in UGT2B17 Gene Deletion Subjects

Testosterone Metabolism by Aldoketoreductases. Cytosolic fraction, isolated from liver tissues of UGT2B17 deletion carriers (two males and one female), were used for the aldoketoreductase (AKR) activity. AKR activity assay was performed in a reaction buffer (100 μL) containing 100 mM sodium phosphate buffer (pH 7.4), 1 mM EDTA, and 10 μM substrate (testosterone or 5β-DHT). The sample was vortex mixed and preincubated at 37°C for 5 minutes before initiating the reaction by adding NADPH cofactor and performing the time-dependent product formation assay for 0, 5, 10, 15, 30, 45, and 60 minutes. The samples were mixed and centrifuged at 4°C at 3200g (5 minutes). The supernatant was collected and diluted twofold with 0.1% formic acid, and analysis of testosterone, 5β-DHT and 3α,5β-tetrahydrotestosterone (3α,5β-THT) was conducted using an optimized LC-MS/MS method on Xevo TQXS instrument (Waters, Milford, MA) (Supplemental Table 1).

Glucuronidation of Reduced-Testosterone Metabolites. Glucuronidation assay of the metabolites formed by AKRs was performed in the recombinant human UGT2Bs (10 μg/ml, final protein concentration). The reaction buffer consists of 100 mM phosphate buffer (pH 7.4), 5 mM MgCl$_2$, alamethicin (0.1 mg/mL), and BSA (0.02%). 5β-DHT and 3α,5β-THT (1 μM) were added to the reaction mixture, which was incubated with alamethicin in ice for 15 minutes to allow the pore formation. The reaction was performed for 30 minutes at 37°C after adding UDP-glucuronic acid (2.5 mM). Ice-cold acetonitrile containing internal standard (epitestosterone glucuronide) was used for quenching the reaction, followed by centrifugation at 2000g, 4°C (5 minutes). The supernatant was mixed with 0.1% formic acid 1:1 (v/v) to reduce the organic content and analyzed by LC-MS/MS to quantify the substrate depletion and the formation of the corresponding glucuronide metabolite using the parameters provided in Supplemental Table 1.

Effect of UGT2B17 Variability on in Vitro Metabolism of Testosterone in Human Hepatocytes. We first identified four cryopreserved hepatocyte lots (two high and two low UGT2B17 expressing) based on targeted proteomics experiment as described previously (Basit et al., 2018). The selected hepatocytes ($n = 4$) were thawed for at 37°C for 60–90 seconds and resuspended in 12 mL hepatocyte thawing media previously warmed to 37°C. The hepatocytes were centrifuged at room temperature at 100g for 5 minutes. The supernatant was discarded without disturbing the cell pellet, and cells were resuspended in 3 mL of HI media. Cell count was carried out using Nexcelom Bioscience Cellometer Auto T4 (Lawrence, MA), and the HI media was added to cell suspension to maintain 0.6 × 10^6 cells per mL. Reaction was initiated with the addition of 150 μL of hepatocyte suspension to 150 μL prewarmed HI media containing testosterone (200 μM) in a 24-well plate. The final 0.3-mL sample contained

0.3 million cells, and 100 μM testosterone in each well was incubated for 60 minutes (37°C) at 100 rpm. The reaction was quenched with 0.6 mL of acetonitrile containing internal standard mix. The incubation mixture was transferred to a 1.7-mL tube, mixed vigorously for 1 minute, and centrifuged at 8000g (10 minutes). The supernatant (100 μL) was acidified by 0.1% formic acid (100 μL) and transferred to an LC-MS vial.

Activation of Testosterone by Bacterial β-Glucuronidases

Ex Vivo Fecal Deconjugation of Testosterone Glucuronide. The glucuronide deconjugation assay was performed using a previously optimized protocol (Ervin et al., 2019). In brief, the reaction mixture containing 10 μL of 25 nM HEPES buffer (pH 6.5), 25 mM NaCl, 5 μL fecal samples (0.1 mg/mL protein), and 30 μL water, was preincubated at 37°C for 5 minutes. The substrate (5 μL TG, 1 μM) was added and incubated for 30 minutes at 37°C. The purified *Eubacterium eligens* GUS (10 μg/mL) was used as a potential positive control in this assay as it universally metabolizes multiple glucuronide substrates (Pollet et al., 2017). The reaction was quenched by adding ice-cold acetonitrile containing testostosterone-d3, 25 nM (internal standard), and the conjugated and deconjugated testosterone were analyzed using an optimized LC-MS/MS method (Basit et al., 2018) with a few modifications shown in Supplemental Table 1.

Screening of Bacterial β-Glucuronidases for the Deconjugation of Testosterone Glucuronide. To identify the role of individual GUS capable of TG deconjugation, we performed the assay using 10 different GUS enzymes using optimized final enzyme concentrations and pH conditions provided in Supplemental Table 2. The reaction containing 20 μl assay buffer, 10 μl enzyme (various concentrations provided in Supplemental Table 2), and 20 μl substrate (50 μM, final 20 μM) in 50 μl of total volume was carried out at 37°C (30 minutes). The variable final enzyme concentrations were selected based on the relative activities of these enzymes against the standard GUS substrate, p-nitrophenol glucuronide (Pollet et al., 2017). The reaction was quenched with 100 μl of the ice-cold acetonitrile containing testosterone-d3. The samples were vortex mixed to allow for mechanical lysis and centrifuged at 13,000g for 10 minutes (4°C). The supernatant (100 μl) was transferred to an LC-MS vial for the analysis by SCIEX 6500 MS (Framingham, MA) coupled with Waters Acquity UPLC (Waters) (Supplemental Table 3). The testosterone concentration was determined using a standard curve (range, 0.1–50 ng/ml).

TG Disappearance with Time in the Presence of GUS Enzymes. The in vitro TG disappearance assay by GUS enzymes isolated from *Escherichia coli* (E. coli) and *E. eligens* was conducted at 37°C in 50 μl total reaction mixture containing 10 μl of incubation buffer (50 mM HEPES, 50 mM NaCl buffer, pH 6.5), 10 μl of GUS enzyme (E. coli and E. eligens diluted to 5 nM, final concentration of 1 nM), and 30 μl of substrate (final concentration, 10 μM) . The reaction was quenched at 5, 10, 15, 20, 30, 45, 60, 75, and 90 minutes after the start of incubation with acetonitrile containing testosterone-d3 as internal standard. The samples were centrifuged and analyzed using the protocol described above. TG disappearance rate (0 minutes versus individual timepoints) was compared using ANOVA followed by Dunnett's T3 multiple comparisons test (*P < 0.05, **P < 0.01, ***P < 0.001).

In Vivo Confirmation of AKR Pathway

Untargeted Metabolomics Analysis of Serum Samples with Oral Testosterone Dosing in Man. Untargeted metabolomics analysis was performed of the serum samples from healthy men participating in an oral testosterone PK study approved by the Institutional Review Board of the University of Washington, Seattle, WA (Amory and Bremner, 2005). All subjects provided written consent for the participation. The serum samples were pooled from all timepoints after a single oral dose (800 mg) of testosterone in oil administered to men (n = 7). Predose-testosterone administration samples were used as controls. Testosterone and its metabolic products were extracted using protein precipitation by ice-cold methanol containing internal standard mix (deuterated steroids) followed by a solid-phase extraction method using C18 hydrophilic-lipophilic balance cartridges (Waters). Briefly, serum samples (200 μL) were transferred to 1.5-mL tubes, and protein precipitation was performed using fivefold higher volume of the internal standard mix. Samples were vortex mixed and centrifuged at 5000g for 10 minutes (4°C). The supernatant was dried under nitrogen evaporator in a glass tube, and the residue was redissolved in 2 mL of 5% methanol containing 0.1% formic acid. The solid-phase extraction cartridges were activated by 2 mL methanol and conditioned by 2 mL 0.1% formic acid before sample (2 mL)

loading. The flow-through was discarded, and the samples were washed with 1 mL of 5% methanol. Analytes were eluted with methanol (2 mL) in a glass tube and dried using a nitrogen evaporator. The reconstituted sample in 0.1 mL 10% acetonitrile was transferred to an LC-MS vial.

The extracted metabolomic samples were analyzed in DDA mode by LC-MS (EASY-nLC 1200 and Q-Exactive HF MS; Thermo Fisher Scientific). Sample was loaded onto a C18 trap column (100 μm × 2 cm, 5 μm, Acclaim PepMap) and desalted for 10 minutes with 0.1% formic acid. The trapped sample was then eluted through a C18 column (Thermo Scientific PepMap; 50 μm × 15 cm, 2 μm). The metabolites were separated with 0.3 μL/min mobile phase using the following gradient condition: 0.0–5.0 minutes (10% B), 5.0–45 minutes (10%–40% B), 45–65 minutes (40%–80% B), 65–69.0 minutes (80% B), and then equilibrated back to 10% B for 10 minutes. Metabolites were detected in DDA mode, where the top ten most intense ions from the MS1 scan were selected for the fragmentation by collision-induced dissociation. The survey scans of metabolites were performed in Orbitrap from 100 to 1000 m/z (resolution of 120,000 at 200 m/z) with a 3×10^6 ion count target and the maximum injection time of 100 milliseconds. The MS/MS resolution was set to 15,000 with an AGC target of 1×10^5 and an isolation window of 1.6 m/z. The collision energy was 27 eV. The untargeted metabolomics data were analyzed using open XCMS online (https://xcmsonline.scripps.edu/), where, the pairwise analysis was performed to compare the metabolomics difference between the groups.

Results

Association of UGT2B17 Gene Deletion with the Liver Proteome in Man. Global proteomics analysis of postmitochondrial (S9) fraction of liver tissue from individuals harboring UGT2B17 deletion and high-expresser genotypes revealed a significant effect of UGT2B17 on hepatic metabolism pathways. We quantified a total of 1002 proteins in the study, with a stringent criterion of a minimum two peptides and at least one unique peptide per protein. 949 proteins were common in the deletion and expresser subjects, whereas 14 and 39 proteins were unique to each group, respectively (Fig. 2A). The principal component analysis and OPLS-DA confirmed the clustering of the samples into two groups (Fig. 2B). Eighty-four proteins were significantly upregulated in UGT2B17 deletion subjects, whereas 89 proteins were significantly downregulated (Fig. 2C; Supplemental Fig. 1). STRING analysis of the upregulated proteins revealed that most of these proteins are associated with oxidoreductase pathways, including AKRs and aldehyde dehydrogenase, e.g., AKR1D1, AKR1C4, AKR1A1, and AKR7A3 were significantly upregulated (Fig. 2D). These proteins play important roles in steroid and bile acid biosynthesis and metabolism (Penning et al., 2019). We also observed that UGT2B7 was significantly upregulated in the UGT2B17 deletion group.

Confirmation of Alternate Testosterone Metabolism Pathways in UGT2B17 Deletion Subjects. Clinical pharmacokinetics data suggest that testosterone is primarily metabolized to androstenedione, AG, EtioG, and TG in adult men (Basit et al., 2018). Interestingly, in UGT2B17 deletion subjects, AKR1D1, AKR1C4, and UGT2B7 enzymes were upregulated, suggesting a major role of these alternate pathways in testosterone disposition in the setting of UGT2B17 gene deletion. These data suggest metabolic switching in UGT2B17 gene deletion subjects, leading to conversion of testosterone to 5β-DHT by AKR1D1, which is subsequently metabolized to 3α,5β-THT by AKR1C4 (Chen et al., 2011). Further, 3α,5β-THT is glucuronidated at 3α-position by another UGT isoform, UGT2B7, which is subsequently eliminated into the urine. The in vitro AKR assay in the liver cytosol confirmed the formation of 5β-DHT from testosterone and 3α,5β-THT from 5β-DHT in a time-dependent manner (Fig. 3; Supplemental Fig. 2). 5β-DHT is selectively glucuronidated by UGT2B17, whereas glucuronidation of 3α,5β-THT at 3-position and 17-position is mediated by UGT2B7 and UGT2B17, respectively (Fig. 3, D and E). Therefore, the major route of THT glucuronidation in UGT2B17 deletion subjects is through 3-glucuronidation via UGT2B7.
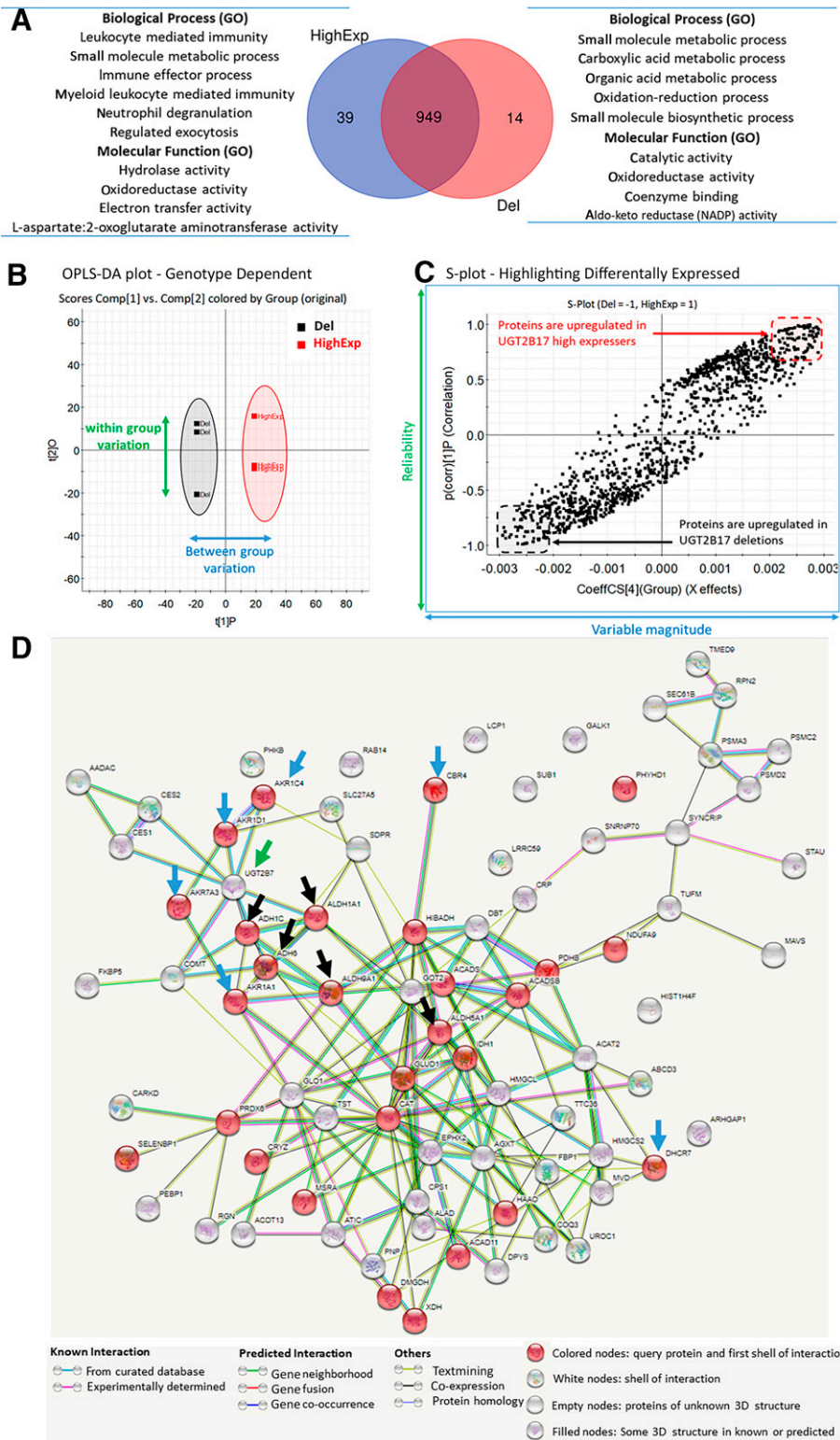
Fig. 2. Untargeted proteomics data of the postmitochondrial (S9) fractions isolated from the liver tissue of the UGT2B17 deletion subjects (Del) versus UGT2B17 high expressers (HighExp). The Venn diagram represents the number of proteins identified in both the groups and the biological processes and molecular functions associated with significantly up-regulated proteins (A). OPLS-DA analysis on the liver proteome shows clustering of individual samples between the deletion and the high-expresser groups (B). The S-plot from OPLS-DA model highlights the differentially expressed proteins in both the groups (C). Protein interactome analysis by STRING analysis of the upregulated proteins in UGT2B17 deletion (D). Significantly upregulated proteins in UGT2B17 gene deletion individuals are associated with aldoketoreductases [AKR1D1, AKR1C4, AKR1A1, AKR7A3, CBR4, and dehydrocholesterol reductase (DHCR)-7; indicated by blue arrows], aldehyde dehydrogenase pathways [aldehyde dehydrogenase (ALDH)-1A1, ALDH5A1, ALDH9A1, ADH1C, and ADH6; indicated by black arrows], and UGT2B7 (indicated by green arrow). The protein interactome of the downregulated proteins is presented in Supplemental Fig. 1.

Testosterone metabolism in human hepatocytes also confirmed high activity of AKR1D1 and AKR1C4 in the low-UGT2B17 expressers. The AKR activities were higher in the hepatocytes with low UGT2B17 activity (Supplemental Fig. 3).

In Vivo Confirmation of AKR Pathway. The qualitative presence of metabolites highlighting the AKR pathway was confirmed in the serum samples of men who were administered 800 mg of oral testosterone.

The exogenous testosterone led to the formation of AKR-mediated THT glucuronide metabolites that were higher in the serum of men exposed to exogenous testosterone than the control serum, whereas phase I metabolites (DHT and THT) were below the detection limit (Fig. 4).

Activation of Testosterone Glucuronide to Testosterone by Microbial GUS Enzymes. TG-to-testosterone conversion in human fecal samples ex vivo indicates the clinical significance of GUS
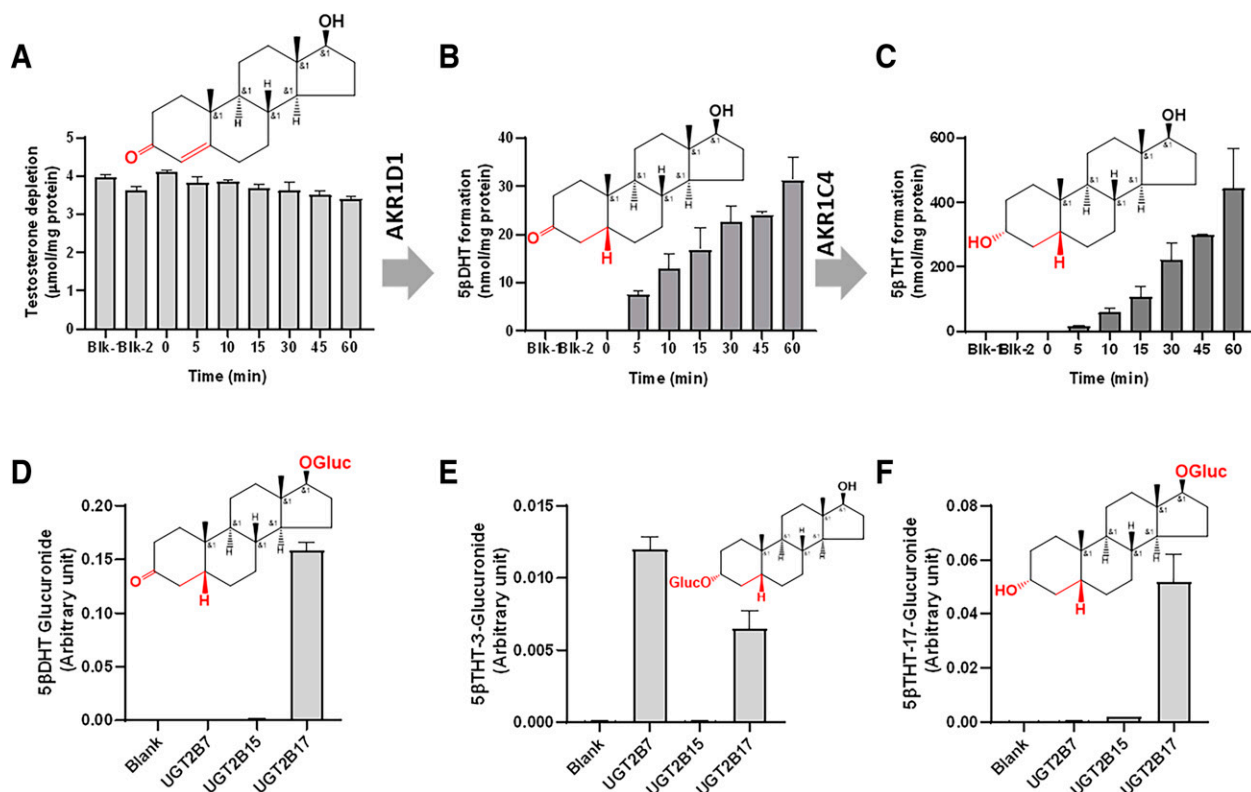
Fig. 3. In vitro testosterone metabolism by aldoketoreductases in liver cytosol samples from the UGT2B17 deletion subjects (A–C) and in the recombinant UGTs (D–F). Testosterone to 5β-DHT and 5β-THT conversion with time by AKR1D1 and AKR1C4 in the human liver cytosol obtained from the UGT2B17 deletion subjects (A–C). Blk-1 and Blk-2 samples do not conatin NADPH and the enzyme, respectively. In vitro glucuronidation of 5β-DHT and 5β-THT using the recombinant human UGT2B enzymes (D–F). Structures of testosterone, 5β-DHT, 3α,5β-THT, 5β-DHT-glucuronide, 3α,5β-THT-3-glucuronide, and 3α,5β-THT-17-glucuronide are shown in (A–F), respectively.

enzymes in testosterone activation in the gastrointestinal tract. Although all ex vivo samples processed TG to testosterone, the sample from male 1 produced more testosterone than did the sample from male 2, with the sample from the female donor being intermediate between the two male samples (Fig. 5A). To identify gut microbial GUS enzymes capable of deconjugating TG to testosterone, we examined 10 distinct GUS enzymes that were previously cloned, expressed, and purified (Ervin et al., 2019). The enzymes employed represented the major gut microbial phyla, as well as the functional clades established for this diverse group of bacterial enzymes (Pollet et al., 2017). We found that all the GUS enzymes studied were able to deconjugate TG back to reactivated testosterone (Fig. 5B), although varying degrees of conversion were observed. These differential abilities to reactivate testosterone from TG were also observed using *E. coli* and *E. eligens* GUS enzymes and time-course studies conducted over 90 minutes, which revealed that *E. coli* GUS exhibited greater TG processing relative to *E. eligens* GUS (Fig. 5, C and D). Taken together, these results show that gut microbial GUS enzymes can reactivate TG to testosterone with varying efficiencies represented in both purified proteins in vitro and fecal extracts ex vivo.

Discussion

To understand the association of UGT2B17 deletion with the liver proteome and metabolome, we performed an untargeted proteomics study comparing liver S9 proteome in individuals harboring UGT2B17 deletion and high-expression genotypes followed by a series of in vitro experiments to interpret the findings. The proteomics data revealed that the upregulated proteins in UGT2B17 deletion subjects were associated with the AKR family. These enzymes catalyze NADPH-dependent

reduction of the steroidal ring at C3, C5, C17, and C20 positions (Rižner and Penning, 2014). We identified that AKR1D1 and AKR1C4 could play critical roles in testosterone metabolism in UGT2B17 nonexpressers. However, this hypothesis needs further in vivo testing if the metabolic switching in UGT2B17 gene deletion subjects changes the rate of elimination or half-life of testosterone. AKR1D1 is selectively expressed in the liver, with minor expression in the fallopian tube and breast, whereas AKR1C4 is ubiquitously expressed across various tissues, with highest expression in the liver (Barski et al., 2008). AKR1D1 is the only human enzyme that stereospecifically reduces Δ^4 double bond of steroidal ring to 5β-dihydro steroid and generates the 5β-reduced dihydrosteroidal metabolites for C19, C21, and C27 steroids, including androgens, glucocorticoids, and bile acids (Nikolaou et al., 2019). Further, AKR1C4 is the major enzyme responsible for the reduction of 3-keto steroids to 3α-hydroxy steroids. These two enzymes work in tandem to metabolize testosterone to 5β-DHT and subsequently to 3α,5β-THT in individuals with UGT2B17 gene deletion. The in vitro activity data at lower testosterone concentration (Supplemental Fig. 2) suggest that the intermediate 5β-DHT is immediately transformed to 3α,5β-THT by AKR1C4 and is unlikely to be accumulated in the liver. 3α,5β-THT is then metabolized by UGT2B7 that is also upregulated in UGT2B17 deletion subjects and is likely excreted as the glucuronide in urine. We have confirmed this metabolic switching through a series of in vitro experiments (Fig. 4). However, it requires in vivo investigations if the perturbation in AKR1D1 activity in UGT2B17 deletion subjects will lead to a higher circulating testosterone. AKRs (AKR1C1-1C4) play important roles in the pathophysiology of prostate, breast, and endometrial cancer (Penning and Byrns, 2009). Similarly, UGT2B17 gene deletion is associated with prostate cancer risk (Kpoghomou et al.,
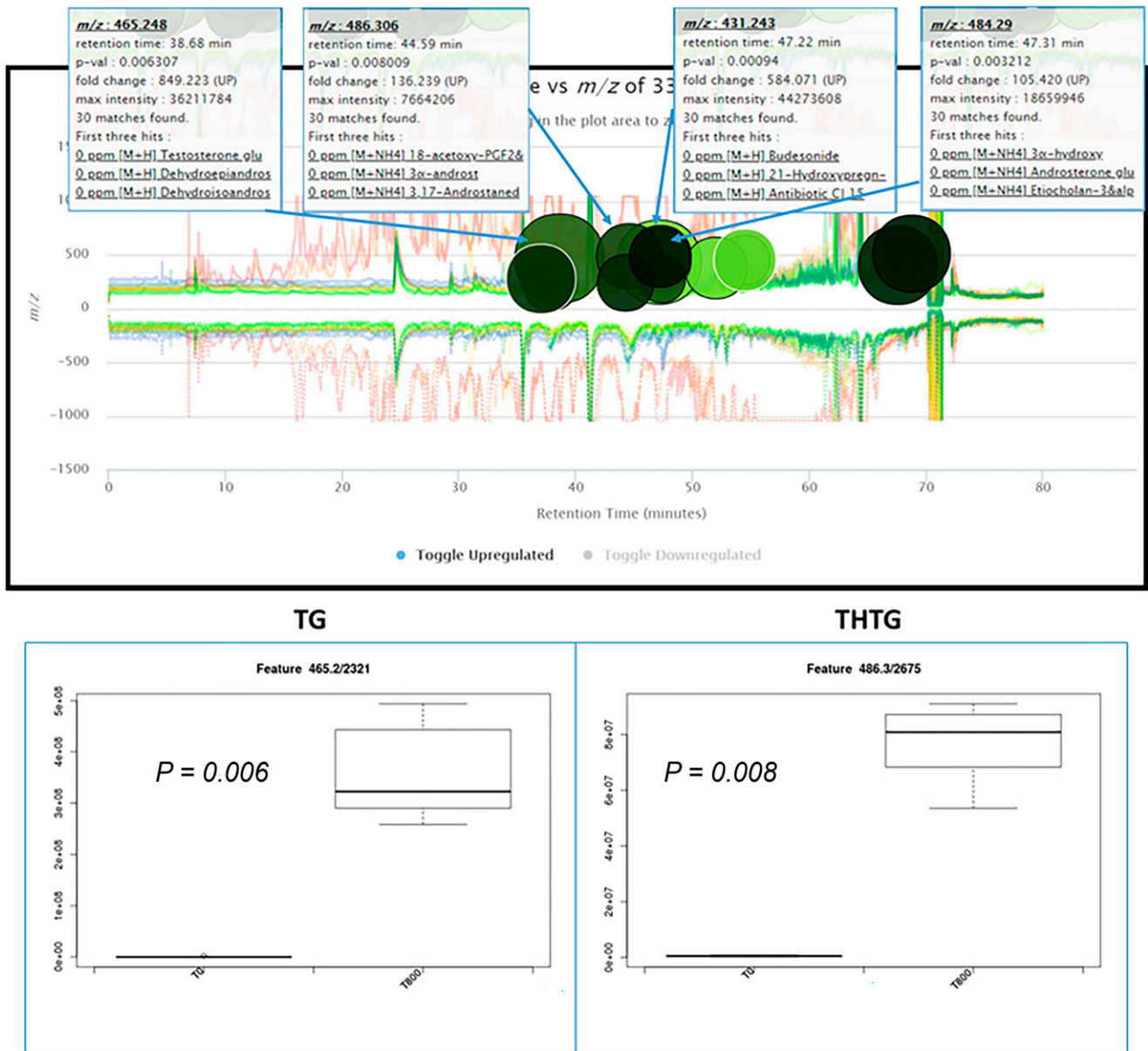
Fig. 4. Metabolic cloud plot representing differentially elevated metabolites in the serum after oral testosterone dosing in men. The cloud plot represents 16 elevated features in human serum sample after oral 800 mg testosterone dose (T800) as compared with the predose (T0) sample (Supplemental Table 4), with $P < 0.01$, fold change > 35, and m/z range 200–600. Visualization represents P value by color intensity (more intense means lower P value) and the fold-change by the radius of the circle. The whisker-box plots show the elevated levels (mass spectrometry peak intensity) of TG (M+H, m/z 465.2482) and $3\alpha,5\beta$-THT-glucuronide (THTG; M+NH$_4$, m/z 486.3060) after oral 800 mg testosterone administration (T800) as compared with the predose sample (T0).

2013; Gauthier-Landry et al., 2015), lower body mass index, higher fat mass (Chew et al., 2011; Zhu et al., 2015), increased bone mineral density, and decreased osteoporotic fractures (Yang et al., 2008; Che et al., 2015). Our findings indicate the mechanistic interplay of AKR and UGT2B17, which needs further investigation to understand the molecular mechanisms. AKR1D1 dysregulation and mutation are linked to bile acid deficiency (Drury et al., 2010). AKR1D1 knockdown in HepG2, Huh7 cells, and human hepatocytes lead to an increased *de novo* lipogenesis and accumulation of triacylglycerol (Nikolaou et al., 2019). The upregulation of AKR1D1 is not well studied, leading to a critical knowledge gap with respect to the pathophysiological role of AKR1D1.

This study also examined the role of gut microbial enzymes in deconjugating TG back to reactivated testosterone. Although the importance of gut microbial GUS enzymes in processing steroid hormone glucuronides

is not novel (Ervin et al., 2019), this is the first analysis of TG hydrolysis by these bacterial proteins. Integration of TG fecal processing rates with proteomics-based GUS enzyme quantification would be a powerful addition to physiologically based pharmacokinetic modeling of testosterone disposition. These mechanistic findings may help understanding the mechanisms of testosterone-associated pathophysiology such as obesity, prostate cancer, lung cancer, endometrial cancer, and doping. Our deconjugation data are supported by recent studies indicating high concentration of free testosterone in colon in both men and mice (Colldén et al., 2019).

In summary, this exploratory study highlights the potential importance of AKR enzymes in testosterone metabolism in UGT2B17 deletion subjects. Our data suggest that AKR1D1, which is expressed selectively in the liver, likely plays an important role in detoxifying excess testosterone in the absence of UGT2B17 activity. Therefore, modulation of AKR1D1
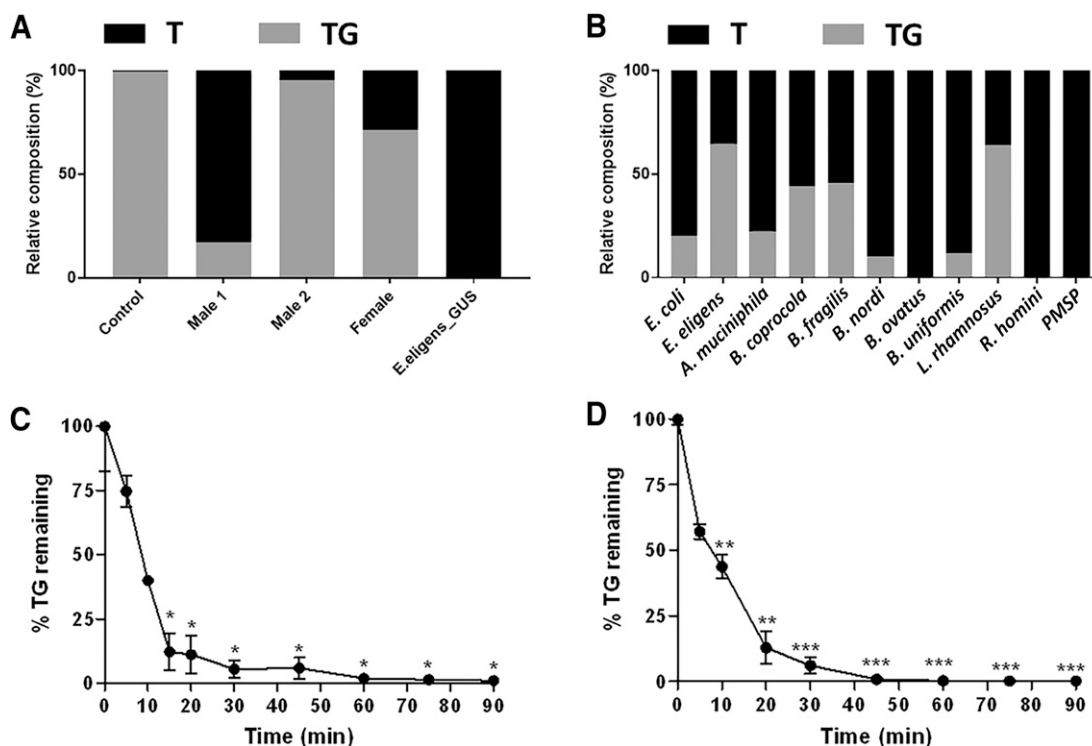
Fig. 5. In vitro bacterial GUS activity toward testosterone glucuronide deconjugation. GUS activity toward testosterone glucuronide in fecal samples at 1 μM TG (A). Deconjugation of TG to testosterone by GUS enzymes from various gut bacterial species at 20 μM TG concentration (B). TG disappearance with time in the presence of GUS enzymes from *E. coli* (C) and *E. eligens* (D) at 10 μM TG concentration. The experiments were performed in triplicates, where percent coefficient of variation (%CV) was within 30% as indicated in (C) and (D). TG disappearance rate [0 minutes versus individual timepoints; (C) and (D)] was compared using ANOVA followed by Dunnett's T3 multiple comparisons test, with $*P < 0.05$; $**P < 0.01$; $***P < 0.001$.

activity in UGT2B17-compromised individuals may cause testosterone-associated side effects. 5β-DHT formed by AKR1D1 activity is rapidly metabolized by AKR1C4 to 3α,5β-THT and subsequently eliminated via glucuronidation. The newer insights on testosterone metabolism are potentially important for explaining the disposition of exogenously administered testosterone and clinical conditions associated with UGT2B17 deletion, e.g., prostate cancer (Gallagher et al., 2007), endometrial cancer (Hirata et al., 2010), chronic lymphocytic leukemia (Gruber et al., 2013), and obesity (Zhu et al., 2015). Further, 5β-DHT, 3α, 5β-THT, and their subsequent metabolites can be added in doping testing to avoid false negative and positive outcomes due to UGT2B17 variability. Similarly, the mechanistic insights on the role of microbiome in testosterone activation in gut can be leveraged in controlling variability in testosterone exposure after exogenous administration and explaining microbiome-associated pathophysiology.

Authorship Contributions

Participated in research design: Basit, Redinbo, Prasad.
Conducted experiments: Basit, Mettu, Li, Jariwala.
Performed data analysis: Basit, Prasad.
Contributed new reagents or analytic tools: Heyward.
Wrote or contributed to the writing of the manuscript: Basit, Amory, Redinbo, Prasad.

References

Amory JK and Bremner WJ (2005) Oral testosterone in oil plus dutasteride in men: a pharmacokinetic study. *J Clin Endocrinol Metab* **90**:2610–2617.

Balhara A, Basit A, Argikar UA, Dumouchel JL, Singh S, and Prasad B (2021) Comparative Proteomics Analysis of the Postmitochondrial Supernatant Fraction of Human Lens-Free Whole Eye and Liver. *Drug Metab Dispos* **49**:592–600.

Barski OA, Tipparaju SM, and Bhatnagar A (2008) The aldo-keto reductase superfamily and its role in drug metabolism and detoxification. *Drug Metab Rev* **40**:553–624.

Basit A, Amory JK, and Prasad B (2018) Effect of Dose and 5α-Reductase Inhibition on the Circulating Testosterone Metabolite Profile of Men Administered Oral Testosterone. *Clin Transl Sci* **11**:513–522.

Bhasin S, Cunningham GR, Hayes FJ, Matsumoto AM, Snyder PJ, Swerdloff RS, and Montori VM (2006) Testosterone therapy in adult men with androgen deficiency syndromes: an endocrine society clinical practice guideline. *J Clin Endocrinol Metab* **91**:1995–2010.

Bhasin S, Cunningham GR, Hayes FJ, Matsumoto AM, Snyder PJ, Swerdloff RS, and Montori VM; Task Force, Endocrine Society (2010) Testosterone therapy in men with androgen deficiency syndromes: an Endocrine Society clinical practice guideline. *J Clin Endocrinol Metab* **95**:2536–2559.

Bhatt K, Basit A, Zhang H, Gaedigk A, Lee S, Claw KG, Mehrotra A, Chaudhry AS, Pearce RE, Gaedigk R, et al. (2018) Hepatic Abundance and Activity of Androgen- and Drug-Metabolizing Enzyme UGT2B17 Are Associated with Genotype, Age, and Sex. *Drug Metab Dispos* **46**:888–896.

Che X, Yu D, Wu Z, Zhang J, Chen Y, Han Y, Wang C, and Qi J (2015) Association of Genetic Polymorphisms in UDP-Glucuronosyltransferases 2B17 with the Risk of Pancreatic Cancer in Chinese Han Population. *Clin Lab* **61**:1905–1910.

Chen M, Drury JE, and Penning TM (2011) Substrate specificity and inhibitor analyses of human steroid 5β-reductase (AKR1D1). *Steroids* **76**:484–490.

Chew S, Mullin BH, Lewis JR, Spector TD, Prince RL, and Wilson SG (2011) Homozygous deletion of the UGT2B17 gene is not associated with osteoporosis risk in elderly Caucasian women. *Osteoporos Int* **22**:1981–1986.

Colldén H, Landin A, Wallenius V, Elebring E, Fändriks L, Nilsson ME, Ryberg H, Poutanen M, Sjögren K, Vandenput L, et al. (2019) The gut microbiota is a major regulator of androgen metabolism in intestinal contents. *Am J Physiol Endocrinol Metab* **317**:E1182–E1192.

Drury JE, Mindnich R, and Penning TM (2010) Characterization of disease-related 5beta-reductase (AKR1D1) mutations reveals their potential to cause bile acid deficiency. *J Biol Chem* **285**:24529–24537.

Ervin SM, Li H, Lim L, Roberts LR, Liang X, Mani S, and Redinbo MR (2019) Gut microbial β-glucuronidases reactivate estrogens as components of the estrobolome that reactivate estrogens. *J Biol Chem* **294**:18586–18599.

Gallagher CJ, Kadlubar FF, Muscat JE, Ambrosone CB, Lang NP, and Lazarus P (2007) The UGT2B17 gene deletion polymorphism and risk of prostate cancer. A case-control study in Caucasians. *Cancer Detect Prev* **31**:310–315.

Gauthier-Landry L, Bélanger A, and Barbier O (2015) Multiple roles for UDP-glucuronosyltransferase (UGT)2B15 and UGT2B17 enzymes in androgen metabolism and prostate cancer evolution. *J Steroid Biochem Mol Biol* **145**:187–192.

Gruber M, Bellemare J, Hoermann G, Gleiss A, Porpaczy E, Bilban M, Le T, Zehetmayer S, Mannhalter C, Gaiger A, et al. (2013) Overexpression of uridine diphospho glucuronosyltransferase 2B17 in high-risk chronic lymphocytic leukemia. *Blood* **121**:1175–1183.

Hirata H, Hinoda Y, Zaman MS, Chen Y, Ueno K, Majid S, Tripsas C, Rubin M, Chen LM, and Dahiya R (2010) Function of UDP-glucuronosyltransferase 2B17 (UGT2B17) is involved in endometrial cancer. *Carcinogenesis* **31**:1620–1626.

Jakobsson J, Ekström L, Inotsume N, Garle M, Lorentzon M, Ohlsson C, Roh HK, Carlström K, and Rane A (2006) Large differences in testosterone excretion in Korean and Swedish men are strongly associated with a UDP-glucuronosyl transferase 2B17 polymorphism. *J Clin Endocrinol Metab* **91**:687–693.

Juul A, Sørensen K, Aksglaede L, Garn I, Rajpert-De Meyts E, Hullstein I, Hemmersbach P, and Ottesen AM (2009) A common deletion in the uridine diphosphate glucuronyltransferase (UGT) 2B17 gene is a strong determinant of androgen excretion in healthy pubertal boys. *J Clin Endocrinol Metab* **94**:1005–1011.19088161

Kpoghomou MA, Soatiana JE, Kalembo FW, Bishwajit G, and Sheng W (2013) UGT2B17 Polymorphism and Risk of Prostate Cancer: A Meta-Analysis. *ISRN Oncol* **2013**:465916.

Li CY, Basit A, Gupta A, Gáborik Z, Kis E, and Prasad B (2019) Major glucuronide metabolites of testosterone are primarily transported by MRP2 and MRP3 in human liver, intestine and kidney. *J Steroid Biochem Mol Biol* **191**:105350.

Li CY, Gupta A, Gáborik Z, Kis E, and Prasad B (2020) Organic Anion Transporting Polypeptide-Mediated Hepatic Uptake of Glucuronide Metabolites of Androgens. *Mol Pharmacol* **98**:234–242.

Mazer N, Bell D, Wu J, Fischer J, Cosgrove M, and Eilers B; BS, RN (2005) Comparison of the steady-state pharmacokinetics, metabolism, and variability of a transdermal testosterone patch versus a transdermal testosterone gel in hypogonadal men. *J Sex Med* **2**:213–226.

Nikolaou N, Gathercole LL, Marchand L, Althari S, Dempster NJ, Green CJ, van de Bunt M, McNeil C, Arvaniti A, Hughes BA, et al. (2019) AKR1D1 is a novel regulator of metabolic phenotype in human hepatocytes and is dysregulated in non-alcoholic fatty liver disease. *Metabolism* **99**:67–80.

Penning TM and Byrns MC (2009) Steroid hormone transforming aldo-keto reductases and cancer. *Ann N Y Acad Sci* **1155**:33–42.

Penning TM, Wangtrakuldee P, and Auchus RJ (2019) Structural and Functional Biology of Aldo-Keto Reductase Steroid-Transforming Enzymes. *Endocr Rev* **40**:447–475.

Pollet RM, D'Agostino EH, Walton WG, Xu Y, Little MS, Biernat KA, Pellock SJ, Patterson LM, Creekmore BC, Isenberg HN, et al. (2017) An Atlas of β-Glucuronidases in the Human Intestinal Microbiome. *Structure* **25**:967–977.e5.

Rane A and Ekström L (2012) Androgens and doping tests: genetic variation and pit-falls. *Br J Clin Pharmacol* **74**:3–15.

Rižner TL and Penning TM (2014) Role of aldo-keto reductase family 1 (AKR1) enzymes in human steroid metabolism. *Steroids* **79**:49–63.

Schlich C and Romanelli F (2016) Issues Surrounding Testosterone Replacement Therapy. *Hosp Pharm* **51**:712–720.

Schulze JJ, Lundmark J, Garle M, Ekström L, Sottas PE, and Rane A (2009) Substantial advantage of a combined Bayesian and genotyping approach in testosterone doping tests. *Steroids* **74**:365–368.

Schulze JJ, Lundmark J, Garle M, Skilving I, Ekström L, and Rane A (2008) Doping test results dependent on genotype of uridine diphospho-glucuronosyl transferase 2B17, the major enzyme for testosterone glucuronidation. *J Clin Endocrinol Metab* **93**:2500–2506.

Spanos C, Bretherton I, Zajac JD, and Cheung AS (2020) Effects of gender-affirming hormone therapy on insulin resistance and body composition in transgender individuals: A systematic review. *World J Diabetes* **11**:66–77.

Strahm E, Mullen JE, Gårevik N, Ericsson M, Schulze JJ, Rane A, and Ekström L (2015) Dose-dependent testosterone sensitivity of the steroidal passport and GC-C-IRMS analysis in relation to the UGT2B17 deletion polymorphism. *Drug Test Anal* **7**:1063–1070.

Swerdloff RS, Pak Y, Wang C, Liu PY, Bhasin S, Gill TM, Matsumoto AM, Pahor M, Surampudi P, and Snyder PJ (2015) Serum Testosterone (T) Level Variability in T Gel-Treated Older Hypogonadal Men: Treatment Monitoring Implications. *J Clin Endocrinol Metab* **100**:3280–3287.

Szklarczyk D, Franceschini A, Wyder S, Forslund K, Heller D, Huerta-Cepas J, Simonovic M, Roth A, Santos A, Tsafou KP, et al. (2015) STRING v10: protein-protein interaction networks, integrated over the tree of life. *Nucleic Acids Res* **43**:D447–D452.

Tyanova S, Temu T, and Cox J (2016a) The MaxQuant computational platform for mass spectrometry-based shotgun proteomics. *Nat Protoc* **11**:2301–2319.

Tyanova S, Temu T, Sinitcyn P, Carlson A, Hein MY, Geiger T, Mann M, and Cox J (2016b) The Perseus computational platform for comprehensive analysis of (prote)omics data. *Nat Methods* **13**:731–740.

Wilson DM, Kiang TKL, and Ensom MHH (2018) Pharmacokinetics, safety, and patient acceptability of subcutaneous versus intramuscular testosterone injection for gender-affirming therapy: A pilot study. *Am J Health Syst Pharm* **75**:351–358.

Xue Y, Sun D, Daly A, Yang F, Zhou X, Zhao M, Huang N, Zerjal T, Lee C, Carter NP, et al. (2008) Adaptive evolution of UGT2B17 copy-number variation. *Am J Hum Genet* **83**:337–346.

Yang TL, Chen XD, Guo Y, Lei SF, Wang JT, Zhou Q, Pan F, Chen Y, Zhang ZX, Dong SS, et al. (2008) Genome-wide copy-number-variation study identified a susceptibility gene, UGT2B17, for osteoporosis. *Am J Hum Genet* **83**:663–674.

Zhang H, Basit A, Busch D, Yabut K, Bhatt DK, Drozdzik M, Ostrowski M, Li A, Collins C, Oswald S, et al. (2018) Quantitative characterization of UDP-glucuronosyltransferase 2B17 in human liver and intestine and its role in testosterone first-pass metabolism. *Biochem Pharmacol* **156**:32–42.

Zhu AZ, Cox LS, Ahluwalia JS, Renner CC, Hatsukami DK, Benowitz NL, and Tyndale RF (2015) Genetic and phenotypic variation in UGT2B17, a testosterone-metabolizing enzyme, is associated with BMI in males. *Pharmacogenet Genomics* **25**:263–269.

Address correspondence to: Dr. Bhagwat Prasad, Department of Pharmaceutical Sciences, Washington State University, 412 E Spokane Falls Blvd, Spokane, WA 99202. E-mail: bhagwat.prasad@wsu.edu